Analysis of the FLVR motif of SHIP1 and its importance for the protein stability of SH2 containing signaling proteins

Patrick A.H. Ehm[a], Fabiola Lange[a], Carolin Hentschel[a], Anneke Jepsen[a], Nina Nelson[a], Bettina Bettin[a], Christina de Bruyn Kops[b], Johannes Kirchmair[b,1], Marcus Nalaskowski[a] and Manfred Jücker[a¶]

[a] Institute of Biochemistry and Signal Transduction, Center for Experimental Medicine, University Medical Center Hamburg-Eppendorf, Martinistr. 52, 20246 Hamburg, Germany

[b] Center for Bioinformatics (ZBH), Department of Informatics, Faculty of Mathematics, Informatics and Natural Sciences, University of Hamburg, 20146 Hamburg, Germany

[¶]Corresponding author: Manfred Jücker
Tel. +49-40-7410-56339; Fax: +49-40-7410-52904;
E-mail: juecker@uke.de

[1] **Present address:** Department of Chemistry, University of Bergen, N-5020 Bergen, Norway and Computational Biology Unit (CBU), University of Bergen, N-5020 Bergen, Norway

Abstract

Binding of proteins with SH2 domains to tyrosine-phosphorylated signaling proteins is a key mechanism for transmission of biological signals within the cell. Characterization of dysregulated proteins in cell signaling pathways is important for the development of therapeutic approaches. The AKT pathway is a frequently upregulated pathway in most cancer cells and the SH2-containing inositol 5-phosphatase SHIP1 is a negative regulator of the AKT pathway. In this study we investigated different mutations of the conserved FLVR motif of the SH2 domain and putative phosphorylation sites of SHIP1 which are located in close proximity to its FLVR motif. We demonstrate that patient-derived SHIP1-FLVR motif mutations e.g. F28L, and L29F possess reduced protein expression and increased phospho-AKT-S473 levels in comparison to SHIP1 wildtype. The estimated half-life of SHIP1-F28L protein was reduced from 23.2 h to 0.89 h in TF-1 cells and from 4.7 h to 0.6 h in Jurkat cells. These data indicate that the phenylalanine residue at position 28 of SHIP1 is important for its stability. Replacement of F28 with other aromatic residues like tyrosine and tryptophan preserves protein stability while replacement with non-aromatic amino acids like leucine, isoleucine, valine or alanine severely affects the stability of SHIP1. In consequence, a SHIP1-mutant with an aromatic amino acid at position 28 i.e. F28W can rescue the inhibitory function of wild type SHIP1, whereas SHIP1-mutants with non-aromatic amino acids i.e F28V do not inhibit cell growth anymore. A detailed structural analysis revealed that F28 forms hydrophobic surface contacts in particular with W5, I83, L97 and P100 which can be maintained by tyrosine and tryptophan residues, but not by non-aromatic residues at position 28. In line with this model of mutation-induced

instability of SHIP1-F28L, treatment of cells with proteasomal inhibitor MG132 was able to rescue expression of SHIP1-F28L. In addition, mutation of putative phosphorylation sites S27 and S33 adjacent to the FLVR motif of SHIP1 have an influence on its protein stability. These results further support a functional role of SHIP1 as tumor suppressor protein and indicate a regulation of protein expression of SH2 domain containing proteins via the FLVR motif.

Keywords: SHIP1, SH2 domain, FLVR motif, instability

Introduction

Dysregulated proteins in cell signaling pathways represent an important starting point for the establishment of therapeutic approaches. The comprehensive characterization of these signaling networks and identification of relevant proteins acting as regulators to inhibit the growth and survival of the tumor cell are therefore of utmost importance to the understanding of cancer. The PI3K/AKT/mTOR signaling pathway plays a key role in cancer therapy because of its frequent overactivation in most tumors (Kandoth et al., 2013). The inositol phosphatase SHIP1 (src homology 2 domain-containing inositol phosphatase 1) serves as a negative regulator of the PI3K/AKT signaling pathway. In recent years SHIP1 has also been identified as an important tumor suppressor (Horn et al., 2004; Pedersen et al., 2009; Miletic et al., 2010; Brauer et al., 2012; Ehm et al., 2015, Täger et al., 2017).

SHIP1 possesses important functions as a negative regulator of signal transduction in hematopoietic cells. The regulatory function of SHIP1 is mediated by its inositol 5-phosphatase activity, catalyzing dephosphorylation of phosphoinositides (PI) and inositol phosphates (IP) at the D5 position of the inositol ring. Regulation of phosphoinositide- and inositol phosphate-mediated cellular processes by SHIP1 (especially conversion of PtdIns (3,4,5)P_3 to PI(3,4)P_2 and Ins(1,3,4,5)P_4 to Ins(1,3,4)P_3) has been extensively studied (Damen et al., 1996; Drayer et al., 1996; Ware et al., 1996; Odai et al., 1997).

Several experimental data strongly suggest that reduced expression and/or reduced activity of SHIP1 plays an important role in leukemogenesis. In T cell acute lymphoblastic leukemia (T-ALL) expression of full length SHIP1 is frequently down regulated (Lo et al, 2009). Simultaneous deletion of SHIP1 and PTEN in a mouse model led to development of lethal B-cell lymphomas (Miletic et al., 2010). In contrast, deletion of PTEN or SHIP1 alone did not result in malignancy in this animal model (Miletic et al., 2010). PTEN and SHIP1 are apparently cooperative in suppressing B-cell lymphoma. In contrast, lentiviral mediated overexpression of SHIP1 alone in a xenograft transplantation model of acute myeloid leukemia resulted in significantly prolonged survival of the mice compared to control cohort (Täger et al., 2017). Furthermore, expression of SHIP1 is down regulated by BCR–ABL and SHIP1 is barely detectable in BCR/ABL-positive chronic myeloid leukemia (Sattler et al., 1999). In addition, Friend murine leukemia virus leads to activation of Fli-1 and, in turn, suppresses the expression of SHIP1. This is associated with an accelerated development of erythroleukemia in mice (Lakhanpal et al., 2010).

The Src homology 2 (SH2) domain is a sequence-specific phosphotyrosine-binding module present in many signaling proteins. Therefore, recognition and binding of proteins with SH2 domains to tyrosine-phosphorylated signaling proteins is a key mechanism for the transmission of many important biological signals within the cell. The SH2 domain is responsible for cellular localization, substrate recruitment and, in some cases, regulates kinase activity (Filippakopoulos et al., 2009). As such the SH2 domain plays a role in stabilizing the inactive

state of Src-kinase family members, but it also stabilizes the active kinase conformation of Fes (Liu et al., 1993; Filippakopoulos et al., 2008).

Furthermore, mutations in the SH2 domain have been shown to destabilize some signaling proteins and cause various diseases. The kinases Fer (W460), ZAP-70 (P80Q), Jak3 (E481G), ITK (R335W) and BTK (different mutations) show mutations that affect their SH2 domains (Richardson et al., 2009; Matsuda et al., 1999; Candotti et al., 1997; Huck et al., 2009; Lappalainen et al., 2008). These mutations are for the most part not involved in phosphotyrosine binding and lead to instability, reduced half-life, and in consequence, increased protein degradation (Filippakopoulos et al., 2009). As a result, kinase activity is impaired in mutants that destabilize the SH2 domain.

The SH2 domain of SHIP1 is important in the context of recruitment of SHIP1 to the cell membrane, where it binds, for example, to the immunoreceptor tyrosine-based inhibitory motif (ITIM) of the inhibitory receptor Fc gamma receptor IIB (FcγRIIB) and serves as negative regulator of the AKT pathway (Pauls and Marshall, 2017). Mutations of the INPP5D gene (SHIP1) in hematopoietic and lymphoid cells are relatively rare (10 mutations out of 4226 primary tissue samples tested, corresponding to 0.24% of all tested cases) (Forbes et al., 2008). In patients with acute myeloid leukemia (AML), some mutations in the INPP5D gene encoding SHIP1 have been described, thereby implicating mutated SHIP1 in the pathogenesis of AML (Luo et al., 2004; Zhang et al., 2006; Gilby et al., 2007; Brauer et al., 2012). Interestingly, mutations of the INPP5D gene have also been described for large intestine carcinoma (89 out of 2320; 3.84%), melanoma (76 out of 1280; 5.94%) and different other carcinomas in higher numbers (Forbes et al., 2008).

However, the molecular mechanisms of how SHIP1 mutations may impair its function as a tumor suppressor must be further illuminated in detail. Knowledge is particulary limited about mutations of SHIP1 that can lead to the instability of the protein. In this study we analyze mutations and putative phosphorylation sites of SHIP1, which affect its FLVR motif or are located in close proximity to its FLVR motif within the SH2 domain. We demonstrate that SHIP1 FLVR motif mutations derived from patients possess reduced protein expression and shorter half-life. In addition, we have presumably identified FLVR motif flanking phosphorylation sites that are involved in regulation of protein expression.

Material and Methods

Construction of plasmids

LeGO-iG2-Puro^{+} SHIP1 vector was generated as previously described (Ehm et al., 2015). The vector was generated by using modified QuikChange site-directed mutagenesis (Wang and Malcolm, 1999). The LeGO-iG2-Puro+ SHIP1 vector was used as template. The following primer pairs were used:

K24R
K24R-FP: 5′- CTTTCCAGGACAGGCAGGGACGGGAGCTTCCTC-3′
K24R-RP: 5′- GAGGAAGCTCCCGTCCCTGCCTGTCCTGGAAAG-3′

S27A
S27A-FP: 5′- ACAGGCAAGGACGGGGCCTTCCTCGTGCGTGCC-3′
S27A-RP: 5′- GGCACGCACGAGGAAGGCCCCGTCCTTGCCTGT-3′

S27D
S27D-FP: 5′- ACAGGCAAGGACGGGGACTTCCTCGTGCGTGCC-3′
S27D-RP: 5′- GGCACGCACGAGGAAGTCCCCGTCCTTGCCTGT-3′

F28I
F28i-FP: 5′- GGCAAGGACGGGAGCATCCTCGTGCGTGCCAGC-3′
F28i-RP: 5′- GCTGGCACGCACGAGGATGCTCCCGTCCTTGCC-3′

F28V
F28V-FP: 5′- GGCAAGGACGGGAGCGTCCTCGTGCGTGCCAGC-3′
F28V-RP: 5′- GCTGGCACGCACGAGGACGCTCCCGTCCTTGCC-3′

F28A
F28A-FP: 5′- GGCAAGGACGGGAGCGCCCTCGTGCGTGCCAGC-3′
F28A-RP: 5′- GCTGGCACGCACGAGGGCGCTCCCGTCCTTGCC-3′

F28Y
F28Y-FP: 5′- GGCAAGGACGGGAGCTACCTCGTGCGTGCCAGC-3′
F28Y-RP: 5′- GCTGGCACGCACGAGGTAGCTCCCGTCCTTGCC-3′

F28W
F28W-FP: 5′- GGCAAGGACGGGAGCTGGCTCGTGCGTGCCAGC-3′
F28W-RP: 5′- GCTGGCACGCACGAGCCAGCTCCCGTCCTTGCC-3′

L29F
L29F-FP: 5′- AAGGACGGGAGCTTCTTCGTGCGTGCCAGCGAG-3′
L29F-RP: 5′- CTCGCTGGCACGCACGAAGAAGCTCCCGTCCTT-3′

R31Q
R31Q-FP: 5′- GGGAGCTTCCTCGTGCAGGCCAGCGAGTCCATC-3′
R31Q-RP: 5′- GATGGACTCGCTGGCCTGCACGAGGAAGCTCCC-3′

Delta FLVR
Delta FLVR-FP: 5′- GGCAAGGACGGGAGCGCCAGCGAGTCCATC-3′
Delta FLVR-RP: 5′- GATGGACTCGCTGGCGCTCCCGTCCTTGCC-3′

S33A
S33A-FP: 5′- TTCCTCGTGCGTGCCGCCGAGTCCATCTCCCGG-3′
S33A-RP: 5′- CCGGGAGATGGACTCGGCGGCACGCACGAGGAA-3′

S33D
S33D-FP: 5′- TTCCTCGTGCGTGCCGACGAGTCCATCTCCCGG-3′
S33D-RP: 5′- CCGGGAGATGGACTCGTCGGCACGCACGAGGAA-3′

S35A
S35A-FP: 5′- GTGCGTGCCAGCGAGGCCATCTCCCGGGCATAC-3′

S35A-RP: 5′- GTATGCCCGGGAGATGGCCTCGCTGGCACGCAC-3′

S35D
S35D-FP: 5′- GTGCGTGCCAGCGAGGACATCTCCCGGGCATAC-3′
S35D-RP: 5′- GTATGCCCGGGAGATGTCCTCGCTGGCACGCAC-3′

Y40A
Y40A-FP: 5′- TCCATCTCCCGGGCAGCCGCGCTCTGCGTGCTG-3′
Y40A-RP: 5′- CAGCACGCAGAGCGCGGCTGCCCGGGAGATGGA-3′

Y46A
Y46A-FP: 5′- GCGCTCTGCGTGCTGGCTCGGAATTGCGTTTAC-3′
Y46A-RP: 5′- GTAAACGCAATTCCGAGCCAGCACGCAGAGCGC-3′

Lentiviral knockdown
Generation of pseudotyped lentiviruses and transduction were performed as previously described (Metzner et al., 2009). 293-T cells were co-transfected with the plasmids Gag-Pol (HIV-1 GAG/POL), Rev (HIV1gp6), VSV-G env and target vector DNA.
Target cells were seeded at a density of 5×10^5 cells per 6-well. Two ml of fresh culture medium and 2 ml of virus supernatant were added. Transduced cells were selected by addition of puromycin (Sigma-Aldrich) to culture medium for at least 1 week before experiments were carried out.

Western blot analysis and determination of protein half-life
To avoid rapid degradation of cellular proteins due to protease activity, cells were lysed directly in cold 150mM NaCl supplemented with 10% (w/v) trichloroacetic acid (TCA) for 30 minutes. After centrifugation, the supernatant was discarded and the pellet was solved in an appropriate volume of 1x loading buffer. The cell pellet was then sonicated at 4°C. Insoluble particles were separated by centrifugation at 4°C and 13,000 x g for 5 min. The supernatant was transferred to fresh tubes. The protein lysates were stored at -80°C.
Proteins were analyzed by SDS–polyacrylamide gel electrophoresis and transferred to nitrocellulose membrane. As a loading control, Ponceau S staining of the membrane was performed. Subsequently, the membrane was hybridized with either rat anti-HA High Affinity antibody (Roche), mouse anti-SHIP1 antibody (P1C1) or mouse anti-HSC70 antibody (B-6) (both Santa Cruz). Further antibodies used were anti-mouse IgG HRP-conjugated, anti-rabbit IgG HRP-conjugated (both Cell Signaling) and goat anti-rat IgG HRP (Santa Cruz).
Protein half-life was determined by treatment with cycloheximide (Sigma-Aldrich) for 0 – 24 hours before lysis and Western blotting. Subsequently, protein expression was quantified using LAS-3000 Imager from Fuji (Raytest). Ponceau S staining was used to normalize the abundance of SHIP1 to the total amount of protein in each lane. Intensity of the Western blot band observed at time point 0h (untreated) was set to 100%. Protein half-life was calculated by the use of GraphPad Prism program. Exponential decay and asymptotic approach to zero were assumed.

RNA isolation, cDNA synthesis and real-time quantitative PCR (qPCR)
Total RNA was isolated with the Direct-Zol RNA MiniPrep Kit (ZYMO Research) following the manufacturer's instruction. First strand cDNA was synthesized with the Promega M-MLV Reverse Transcriptase (Promega) following the manufacturer's instruction.

Sense and antisense oligonucleotide primers for amplification of mRNAs of human SHIP1 and the housekeeping genes GAPDH were designed as followed:

SHIP1 FP: 5′- CCTATGACGTGCCCGACTATGC-3′;
SHIP1 RP: 5′-AGCGGCACAGGGTATTGCAGATGGGTC-3′;
GAPDH-FP: 5′- GAGTCAACGGATTTGGTCGT-3′;
GAPDH-RP: 5′- TTGATTTTGGAGGGATCTCG-3′

Oligonucleotide primers were obtained from MWG. QPCR was performed on LightCycler (Roche).

Determination of cell growth by live cell imaging

For determination of cell growth, 3×10^4 cells were seeded in 200 µl medium per 96 well and allowed to adhere and grow for the indicated time. Cells were incubated during this time at 37 °C in a humidified atmosphere. The live-cell-imaging system IncucyteZoom (Sartorius) enables automated quantification of cell behavior, especially cell growth, over time by automatically collecting and analyzing images at any time.

Cell viability assay

For the Alamar Blue cell viability assay 3×10^4 cells were seeded in 100 µl medium per 96 well and allowed to adhere and grow for the indicated time. Prior to measurement 100 µl medium containing 5 ng/ml resazurin (Sigma-Aldrich) was added to each well. Cells were incubated for 60–240 min at 37 °C in a humidified atmosphere. Fluorescence based absorption was measured at 540 nm on a microplate reader.

Molecular modelling

The structure of SHIP1-wt and the F28L mutant were modelled based on the NMR structures deposited under PDB entry 2YSX. The 20 deposited protein conformations show a moderate degree of flexibility around residue 28, for which reason Figure 6 only shows on (i.e. the first) conformer. The mutation was introduced with the Mutate Residue function in Maestro [Maestro, Schrödinger version 2018-3, New York, NY, 2018]. The protein structures were prepared using the Maestro Protein Preparation Wizard (structure preprocessing with default settings; restrained minimization with the OPLS3e force field and default settings).

Results

Patient derived FLVR-motif mutation F28L leads to reduced SHIP1 protein expression

SHIP1 mutations provide an interesting basis for the functional understanding and analysis of structural elements, such as domains and motifs of this protein. Interestingly, analysis of Cosmic database (https://cancer.sanger.ac.uk/cosmic) revealed a number of SHIP1-mutations derived from leukemia patients and patients with other tumors that either, affect its FLVR motif (residues 28-31) or are located in close proximity to its FLVR motif. These mutations include F28L (AML), L29F (malignant melanoma), L29L (lung carcinoma), R31H (mesothelioma), S33T (ovarian carcinoma), S33S (breast carcinoma), S37P (biliary cancer), R38Q (lung carcinoma), A41T (colon carcinoma), A41V (prostate carcinoma) and R47W (malignant melanoma). In addition, analysis of the PhosphoSite database (Hornbeck et al., 2004) revealed that a number of putative phosphorylation sites (P) and one ubiquitinylation site (Ub) are

located in close proximity to the FLVR motif of SHIP1. These sites include amino acids K24 (Ub), S27 (P), S35 (P), Y40 (P) and Y46 (P) (Figure 1A).

A reduced binding to tyrosine phosphorylated proteins has already been described for the SHIP1-F28L mutation (Brauer et al., 2012). First, TF-1 cells were transduced with control vector, SHIP1 wt, SHIP1-F28L and a mutant with reduced SHIP1 phosphatase activity (Y643H). The cells were then selected with puromycin. Subsequently, protein lysates were prepared by TCA precipitation and analyzed by Western Blot.

The results in Figure 1B confirm that F28L mutant, unlike SHIP1 wild type and SHIP1-Y643H mutant, shows lower SHIP1 expression. Only after a very long exposure SHIP1-F28L protein was detected.

In order to investigate whether the reduction of SHIP1 expression takes place at the transcriptional or translational level, mRNA level of SHIP1 was determined by RT-qPCR. The results of this experiment are shown in Figure 1C. Interestingly, SHIP1 mRNA level of SHIP1-wt, SHIP1-F28L and SHIP1-Y643H are comparable. Thus, the reduction of SHIP1 expression seems to occur at the protein level.

The next step was to investigate whether the SHIP1-F28L mutant is actively degraded. For this purpose, cells expressing SHIP1-F28L were inhibited with the Src kinase inhibitor PP2 or with an inhibitor for proteasomal degradation, MG-132. The results in Figure 1D show that degradation of SHIP1-F28L mutant can be reduced by treatment with PP2 or MG-132 compared to DMSO-treated cells.

An aromatic amino acid at position 28 of SHIP1 is important for its protein stability

The next step was to investigate the influence of aromatic amino acids on the stability of the SHIP1 protein at position 28. For mimicking F28, the structurally similar amino acids tyrosine and tryptophan were selected. In addition, to simulate L28, SHIP1 mutants with the amino acids alanine, valine and isoleucine were generated. Also, a mutant was generated which lacks the complete FLVR motif (ΔFLVR) of SHIP1. Together, control vector, SHIP1-wt and SHIP1-mutant DNA were transduced into H1299 cells. Cells were selected with puromycin. Subsequently, protein lysates were prepared by TCA precipitation and analyzed by Western Blot.

SHIP1-F28Y (158%±15.5%) and F28W (125.4%±8.9%) had a strong expression of SHIP1 even stronger than that of the SHIP1-wt (Figure 2A). In contrast, SHIP1 mutations F28L (1%±0.5%), F28I (7.2%±2.8%), F28V (8.5%±3.5%), F28A (7.4%±1.0%), and ΔFLVR (16.4%±7.0%) showed a markedly reduced SHIP1 expression in comparison to SHIP1-wt.

In addition, cells expressing SHIP1-wt (20.8%±6.8%), F28Y (24.8%±10.9%) and F28W (14.9%±8.9%) showed a marked reduction of AKT phosphorylation (S473) compared to control vector-expressing cells. SHIP1-F28L mutant led to a reduction of AKT phosphorylation (S473) compared to vector control (40.4%±7.0%). In contrast, SHIP1-mutants F28I (88.1%±24.5%), F28V (140.6%±22.9%), F28A (106.6%±23.3%) and ΔFLVR (116.9%±12.6%) showed marginal or no changes of phosphorylation of AKT-S473 compared to vector control.

In order to check whether the SHIP1 mRNA quantity of all mutants is comparable, SHIP1 mRNA was determined by RT-qPCR. The results of this study are shown in Figure 2C. The SHIP1 mRNA amounts of SHIP1-wt and the examined SHIP1 mutants were comparable. So in consequence, an aromatic amino acid at position 28 of SHIP1 is important for its protein stability

Influence of FLVR motif flanking modification sites on protein stability of SHIP1

The next step was to investigate the effect of further SHIP1 mutations within the FLVR motif (L29F and R31Q). In addition, the effects of putative phosphorylation sites S27, S33, S35, Y40 and Y46 were investigated.

For this purpose, pseudo-phosphorylation (S→D) and pseudo-dephosphorylation mutants (S→A) were prepared. Furthermore, the putative ubiquitinylation site K24 was examined more closely. Here, a mutant was created that impeded ubiquitinylation at position 24 (K→R). Together, control vector, SHIP1-wt and SHIP1-mutants were transduced into H1299 cells. Cells were selected with puromycin. Subsequently, protein lysates were prepared by TCA precipitation and analyzed by Western Blot.

The results in Figure 3A and B show that SHIP1 mutants K24R (121%±10.5%), S27A (143%±16.5%), and S33D (190.5%±49.4%) had enhanced SHIP1 expression compared to SHIP1-wt. The mutants S35A (78.7%±8.4%) and S35D (87.2%±3.8%) showed a slightly lower SHIP1 expression compared to SHIP1 wt. In contrast, SHIP1 mutants S27D (7.1%±2.9%), F28L (1.4%±0.4%), L29F (5.2%±2.4%), R31Q (5%±3.1%), S33A (28.2%±6.3%), Y40A (28.5%±6.9%) and Y46A (23.1%±1.6%) showed a marked reduced expression compared to SHIP1-wt.

K24R mutant showed the strongest reduction in phosphorylation of AKT-S473 (5.1%±3.5%) compared to vector control. In comparison to vector control, wild-type (18.6%±9.3%), S27A (22.2%±14.5%), S27D (35.8%±6.8%), F28L (40.4%±11.6%), L29F (59.8%±21.2%), R31Q (73%±5.9%), S33A (36.7%±20.2%), S33D (23%±18.2%), S35A (47.8%±13.3%), S35D (52.6%±14.0%), Y40A (71.1%±20.5%), and Y46A mutant (58.1%±36.3%) reduce the phosphorylation of AKT (S473). Only S27A (22.2%±14.5%) and S33D (23.0%±18.2%), mutants of SHIP1 showed comparable reductions in the phosphorylation of AKT (S473) as could be achieved by SHIP1-wt. The amount of SHIP1-wt mRNA and the mRNA amount of SHIP1 mutants was comparable (Figure 3C). In consequence, mutation of putative phosphorylation sites (S27 and S33) adjacent to the FLVR-motif of SHIP1 have an influence on its protein expression.

Analysis of the growth behavior of cells with FLVR motif mutations

In the next step, the growth behavior of chosen mutants were investigated. First, an Alamar Blue cell viability assay was performed. The results in Figure 4A show that, compared to control vector expressing cells, cells expressing SHIP1-wt (86.9%±1.4%), K24R (74.1%±3.7%), S27A (66%±2.6%), S27D (91%±1.2%), S33A (88.5%±0.5%), S33D (62.2%±1.2%) and F28W mutant (81.5%±1.9%) have significantly lower viability. The

mutants F28L (97.5%±1.4%) and F28V (95.3%±0.9%) show no significant difference in cell viability as compared to control vector expressing cells.

In addition, the growth behavior of control vector, SHIP1-wt, SHIP1-F28L, SHIP1-F28W and SHIP1-K24R expressing H1299 cells was tracked by live cell imaging (IncucyteZoom). For this purpose, the respective cells were seeded and confluence of the cells were monitored for 24 hours.

The results in Figure 4B show that wild-type SHIP1 (89.5%±4.7%), F28W (79.4%±4.0%) and K24R mutant (81.2%±5.2%) had significantly lower cell confluence compared to vector control expressing cells. F28L mutant (100.4%±0.94%) showed comparable cell confluence as the vector control expressing cells.

Moreover the half-life of SHIP1 protein was investigated by using cycloheximide to inhibit protein synthesis. The half-life of SHIP1-F28L mutant in Jurkat (Figure 5A) and TF-1 (Figure 5B) cells was drastically reduced compared to half-life of SHIP1 wild type. So half-life analysis of SHIP1 in Jurkat cells showed a significantly reduced half-life of SHIP1-F28L protein (0.6 hours) compared to half-life of SHIP1-wt protein (4.7 hours). In addition, half-life analysis of SHIP1 in TF-1 cells showed a significantly reduced half-life of SHIP1-F28L protein (0.89 hours) compared to half-life of SHIP1 wild-type protein (23.2 hours).

Discussion

Binding of phosphotyrosine-containing motifs (pY) occur by Src homology 2 (SH2) domains and phosphotyrosine binding domains (PBD). The SH2 domain usually comprises about 100 amino acids and is part of over 100 proteins. It was shown that specificity of the SH2 domain depends on C-terminal residues of the phosphotyrosine (Songyang et al., 1993).

In addition to proteins with FLVR motif, some proteins have a related FLIR/YLLR motifs. Proteins with FLVR motif are e.g. Src, SHIP1 and ABL1. Proteins with FLIR/YLLR motif include Lyn, Grb2, Syk and SH2D1A. These conserved motifs are usually preceded by a glycine and a serine or threonine. A glutamic acid and a serine are often located C-terminal of the FLVR motif. Thus, the eight amino acid residue motif G (S / T) FLVR (E / D) S defines the amino acid sequence essential to the recognition of tyrosine-phosphorylated proteins (Hidaka et al., 1991).

The arginine in the FLVR motif of SH2 domains is the only amino acid of that motif that is directly involved in binding of phosphotyrosine. Accordingly, it has previously been shown that an arginine-mutant of the FLVR motif can inhibit the binding to phosphotyrosine residues (Mayer et al., 1992). Within the scope of this work, the analysis of the Cosmic database (https://cancer.sanger.ac.uk/cosmic; Forbes et al., 2011) revealed a number of mutations observed in leukemia patients as well as in patients with other tumors, which affect the FLVR motif (residues 28-31) or located in close proximity to the FLVR motif of SHIP1. These include the mutations F28L (AML), L29F (malignant melanoma), L29L (lung carcinoma), S33T (ovarian carcinoma), R38Q (lung carcinoma), A41T (colon carcinoma), A41V (prostate carcinoma) and R47W (malignant melanoma). Reduced binding to tyrosine phosphorylated proteins has been described for SHIP1-F28L mutation (Brauer et al., 2012). Furthermore, it was

shown that the expression of SHIP1-F28L in K562 CML cells, compared to expression of SHIP1-wt, can no longer reduce the phosphorylation of AKT-S473 and AKT-T308 (Yang et al., 2009).

The results of this work show that SHIP1 mutations, affecting the FLVR motif of SHIP1 (F28L, L29F and R31Q) can lead to a reduced expression of SHIP1 at the protein level. We also showed that the expression of SHIP1-wt and SHIP1 mutants of the FLVR motif are comparable at the transcriptional level. Closer examination of the SHIP1-F28L mutation revealed that amino acids with aromatic residues at position 28 of SHIP1 (F28Y and F28W) preserve the stability of the protein, whereas the replacement of an aromatic by a non-aromatic amino acid (F28L, F28I, F28V and F28A) severely affects protein stability. From a more detailed structural analysis it has become clear that F28 of SHIP1 likely has no direct influence on phosphotyrosine-binding because the phenylalanine is too far away from the location of the bound phosphotyrosine (the distance between C^{ζ} of F28 and C^{ζ} of R31 is approximately 15 Å).

However, F28 forms hydrophobic surface contacts in particular with, W5, I83, L97 and P100. While both tyrosine and tryptophan at position 28 are able to maintain these interactions, replacement of F28 with leucine likely leads to a loss or weakening of these contacts (Figure 6). It is safe to assume that the (partial) elimination of surface contacts has a significant impact on the conformation, flexibility and stability of the SH2 domain that is detrimental to the binding of tyrosine-phosphorylated proteins, as observed previously for SHIP1 (Brauer et al., 2012).

Defective folding could be identified by ubiquitin ligases. Ubiquitin ligases subsequently catalyzes ubiquitination and thus degradation of misfolded proteins (Jackson and Hewitt, 2016). The Sattler group has shown previously that SHIP1 is a relatively long-lasting protein with a half-life of approximately 17 hours in Ba/F3 cells and half-life is reduced to less than 3 hours by the induction of BCR-ABL (Sattler et al., 1999).

In addition, mutations in the SH2 domain have been shown to destabilize some signaling proteins (Fer, ZAP-70, Jak3, ITK and BTK) and cause various diseases (Richardson et al., 2009; Matsuda et al., 1999; Candotti et al., 1997; Huck et al., 2009; Lappalainen et al., 2008). These mutations are for the most part not involved in phosphotyrosine binding and lead to instability, reduced half-life, and in consequence, increased protein degradation (Filippakopoulos et al., 2009). The X-linked lymphoproliferative syndrome is based on mutations in the SH2D1A gene which codes for the SLAM-associated protein (SAP). Two mutations in the SH2D1A gene could be identified that affect the G^{27}SYLLRDS motif (S28R and R32Q) (Morra et al., 2001). Analysis of these two SH2D1A mutants shows that both mutations lead to a significant reduction in half-life compared to wild type (Morra et al., 2001). In addition, it could be shown for this R32Q mutation that binding between SH2 domain of SAP and phosphotyrosine of CD150 is disturbed (Morra et al., 2001).

Examination of point mutations of the F^{168}LVRES (ES) motif of the ABL SH2 domain reveals that ABL mutations R171K, S173C and S175C disrupt phosphotyrosine binding (Mayer et al., 1992). Due to the R171K mutation, the binding of ABL to phosphoproteins is impaired (Mayer et al., 1992). In contrast, both S173C and S175C mutation can only bind to tyrosine phosphorylated proteins at very high concentrations (Mayer et al., 1992). In contrast, ABL mutations V170L, E172Q and E174Q show no changes in phosphotyrosine binding (Mayer et al., 1992).

In addition, analysis of the phosphosite database revealed that a number of putative phosphorylation sites (S27, S33, S35, Y40, and Y46) are located in close proximity to the FLVR motif of SHIP1 (Hornbeck et al., 2004). In addition, a putative ubiquitinylation site (K24) was analyzed. The putative phosphorylation sites are in part highly conserved between the individual representatives of the SH2-containing proteins (Supplement Figure S1).

In particular, the serine at position 33 of SHIP1 can be identified in almost all representatives, with the exception of Syk. Interestingly, we found that protein expression of SHIP1 can be regulated in particular by the amino acids S27 and S33, which flank the FLVR motif of SHIP1. Unexpectedly, pseudophosphorylation of S27 (S27D) resulted in a decreased expression of SHIP1, whereas the pseudophosphorylation of S33 (S33D) resulted in an enhanced expression of SHIP1. In principle it is known that phosphorylation of proteins can initiate protein degradation. Thus, phosphorylation of the so called "phosphodegrone", a short linear motif, generates a surface binding site for ubiquitin ligases (Holt et al., 2012). On the other hand, it has been shown that phosphorylation at a specific position can mask a degradation signal (Holt et al., 2012). This degradation signal could lead to an increased degradation of SHIP1 by the pseudo-dephosphorylation mutant S33A. In addition, it is also conceivable that the added phosphate group impairs the binding of phosphotyrosine-containing proteins to the arginine of the FLVR motif. The tyrosine kinase Syk has two functionally important SH2 domains. The N-terminal SH2 domain possesses a YLLR (FLIR) motif and the C-terminal SH2 domain has a FLIR sequence. The N-terminal SH2 domain of Syk contains serine 44 ($YLLRQS^{44}$) in the immediate vicinity of the FLIR motif. There is no directly adjacent serine in the C-terminal SH2 domain of Syk. However, it has been shown that the SH2 domain forms a loop, which takes S202 in close proximity to the FLIR motif of the SH2 domain (Bohnenberger, 2013). Analysis of the functional importance of these putative Syk phosphorylation sites revealed that following B-cell receptor stimulation, the pseudophosphorylation mutant S202E for the most part prevented calcium ion influx and the pseudophosphorylation mutant S44E completely prevented calcium ion influx (Bohnenberger, 2013).

Interestingly, a more detailed investigation of the putative SHIP1 ubiquitinylation site K24 showed a strong influence on the phosphorylation status of AKT (Figure 3). Accordingly, the de-ubiquitinylation mutant K24R led to an increase in the expression of SHIP1 in comparison to the expression of SHIP1 wild-type. Consequently, an associated strong reduction in the phosphorylation of AKT-S473 was observed. This reduction in the phosphorylation of AKT-S473 was correspondingly greater than the reduction of the phosphorylation of AKT-S473 that could be achieved by the expression of the SHIP1 wild-type. It has previously been shown for PTEN that lysine at position 66 also exerts an influence on regulation of its expression status. Accordingly, the de-ubiquitination mutant K66R led to an increased expression of PTEN and a concomitant reduction in the phosphorylation of AKT S473 and T308 (Gupta and Leslie, 2016). Due to the lack of endogenous expression of PTEN in H1299 cells, the expression of SHIP1 has a direct influence on the phosphorylation of AKT-S473 and moreover on viability and growth of the cells.

Conclusion

In summary, our results demonstrate that SHIP1-FLVR-motif mutations derived from patients reveal reduced protein expression and shorter protein half-life. Especially amino acids with

aromatic residues at position 28 of SHIP1 preserve the stability of the protein, whereas the replacement of an aromatic to a non-aromatic amino acid severely affects stability of the protein. Moreover, we presumably identified FLVR motif flanking phosphorylation sites that allow regulation of protein expression. These results further support a functional role of SHIP1 as tumor suppressor protein.

Abbreviations: PtdIns(3, 4, 5)P_3, phosphatidylinositol-(3, 4, 5)-trisphosphate; PtdIns(3, 4)P_2, phosphatidylinositol-(3, 4)-bisphosphate; SHIP1, src homology 2 domain-containing inositol phosphatase 1

Acknowledgments
We thank Kristoffer Riecken and Boris Fehse for providing the LeGO-iG2-Puro$^+$ vector. We would like to thank Madeleine Glück for technical support. Thanks to the Forschungsinstitut Kinderkrebs-Zentrum Hamburg for financial support to PE, and to the Bergen Research Foundation (BFS; grant no. BFS2017TMT01) for the financial support of JK. This study was supported by a grant from the Erich und Gertrud Roggenbuck-Stiftung to PE und MJ (0424/108).

References

Bohnenberger H. (2013). Regulation of the "spleen tyrosine kinase" Syk in the B-cell antigen receptor signaling pathway. Dissertation/PhD-Thesis. Georg-August-Universität Göttingen.

Brauer H, Strauss J, Wegner W, Müller-Tidow C, Horstmann M, Jücker M. (2012). Leukemia-associated mutations in SHIP1 inhibit its enzymatic activity, interaction with the GM-CSF receptor and Grb2, and its ability to inactivate PI3K/AKT signaling. Cell Signal. 24(11):2095-101.

Candotti F, Oakes SA, Johnston JA, Giliani S, Schumacher RF, Mella P, Fiorini M, Ugazio AG, Badolato R, Notarangelo LD, Bozzi F, Macchi P, Strina D, Vezzoni P, Blaese RM, O'Shea JJ, Villa A. (1997). Structural and functional basis for JAK3-deficient severe combined immunodeficiency. Blood. 90(10):3996-4003.

Damen JE, Liu L, Rosten P, Humphries RK, Jefferson AB, Majerus PW, Krystal G. (1996). The 145-kDa protein induced to associate with Shc by multiple cytokines is an inositol tetraphosphate and phosphatidylinositol 3,4,5-triphosphate 5-phosphatase. Proc Natl Acad Sci U S A 93:1689-93

Drayer AL, Pesesse X, De Smedt F, Woscholski R, Parker P, Erneux C. (1996). Cloning and expression of a human placenta inositol 1,3,4,5-tetrakisphosphate and phosphatidylinositol 3,4,5-trisphosphate 5-phosphatase. Biochem Biophys Res Commun 225:243-9

Ehm P, Nalaskowski MM, Wundenberg T, Jücker M. (2015). The tumor suppressor SHIP1 colocalizes in nucleolar cavities with p53 and components of PML nuclear bodies. Nucleus. 6(2):154-64.

Filippakopoulos P, Kofler M, Hantschel O, Gish GD, Grebien F, Salah E, Neudecker P, Kay LE, Turk BE, Superti-Furga G, Pawson T, Knapp S. (2008). Structural coupling of SH2-kinase domains links Fes and Abl substrate recognition and kinase activation. Cell. 134(5):793-803.

Filippakopoulos P, Müller S, Knapp S. (2009). SH2 domains: modulators of nonreceptor tyrosine kinase activity. Curr Opin Struct Biol. 19(6):643-9.

Forbes SA, Bhamra G, Bamford S, Dawson E, Kok C, Clements J, Menzies A, Teague JW, Futreal PA, Stratton MR. (2008). The Catalogue of Somatic Mutations in Cancer (COSMIC). Curr Protoc Hum Genet. Chapter 10: Unit 10.11.

Gilby DC, Goodeve AC, Winship PR, Valk PJ, Delwel R, Reilly JT. (2007). Gene structure, expression profiling and mutation analysis of the tumour suppressor SHIP1 in Caucasian acute myeloid leukaemia. Leukemia. 21(11):2390-3.

Gupta A, Leslie NR. (2016). Controlling PTEN (Phosphatase and Tensin Homolog) Stability: A DOMINANT ROLE FOR LYSINE 66. J Biol Chem. 291(35):18465-73.

Hidaka M, Homma Y, Takenawa T. (1991). Highly conserved eight amino acid sequence in SH2 is important for recognition of phosphotyrosine site. Biochem Biophys Res Commun. 180(3):1490-7.

Holt LJ. (2012). Regulatory modules: Coupling protein stability to phopshoregulation during cell division. FEBS Lett. 586(17):2773-7.

Horn S, Endl E, Fehse B, Weck MM, Mayr GW, Jücker M. (2004). Restoration of SHIP activity in a human leukemia cell line downregulates constitutively activated phosphatidylinositol 3-kinase/Akt/GSK-3beta signaling and leads to an increased transit time through the G1 phase of the cell cycle. Leukemia. 18(11):1839-49.

Hornbeck PV, Chabra I, Kornhauser JM, Skrzypek E, Zhang B. (2004). PhosphoSite: A bioinformatics resource dedicated to physiological protein phosphorylation. Proteomics. 4(6):1551-61.

Huck K, Feyen O, Niehues T, Rüschendorf F, Hübner N, Laws HJ, Telieps T, Knapp S, Wacker HH, Meindl A, Jumaa H, Borkhardt A. (2009). Girls homozygous for an IL-2-inducible T cell kinase mutation that leads to protein deficiency develop fatal EBV-associated lymphoproliferation. J Clin Invest. 119(5):1350-8.

Jackson MP, Hewitt EW. (2016). Cellular proteostasis: degradation of misfolded proteins by lysosomes. Essays Biochem. 60(2):173-180.

Kandoth C, McLellan MD, Vandin F, Ye K, Niu B, Lu C, Xie M, Zhang Q, McMichael JF, Wyczalkowski MA, Leiserson MDM, Miller CA, Welch JS, Walter MJ, Wendl MC, Ley TJ, Wilson RK, Raphael BJ, Ding L. (2013). Mutational landscape and significance across 12 major cancer types. Nature. 502(7471):333-339.

Lakhanpal GK, Vecchiarelli-Federico LM, Li YJ, Cui JW, Bailey ML, Spaner DE, Dumont DJ, Barber DL, Ben-David Y. (2010). The inositol phosphatase SHIP-1 is negatively regulated by Fli-1 and its loss accelerates leukemogenesis. Blood. 116(3):428-36.

Lappalainen I, Thusberg J, Shen B, Vihinen M. (2008). Genome wide analysis of pathogenic SH2 domain mutations. Proteins. 72(2):779-92.

Liu X, Brodeur SR, Gish G, Songyang Z, Cantley LC, Laudano AP, Pawson T. (1993). Regulation of c-Src tyrosine kinase activity by the Src SH2 domain. Oncogene. 8(5):1119-26.

Lo TC, Barnhill LM, Kim Y, Nakae EA, Yu AL, Diccianni MB. (2009). Inactivation of SHIP1 in T-cell acute lymphoblastic leukemia due to mutation and extensive alternative splicing. Leuk Res. 33(11):1562-6.

Luo JM, Liu ZL, Hao HL, Wang FX, Dong ZR, Ohno R. (2004). Mutation analysis of SHIP gene in acute leukemia. Zhongguo Shi Yan Xue Ye Xue Za Zhi. 12(4):420-6.

Matsuda S, Suzuki-Fujimoto T, Minowa A, Ueno H, Katamura K, Koyasu S. (1999). Temperature-sensitive ZAP70 mutants degrading through a proteasome-independent pathway. Restoration of a kinase domain mutant by Cdc37. J Biol Chem. 274(49):34515-8.

Mayer BJ, Jackson PK, Van Etten RA, Baltimore D. (1992). Point mutations in the abl SH2 domain coordinately impair phosphotyrosine binding in vitro and transforming activity in vivo. Mol Cell Biol. 12(2):609-18.

Metzner A, Precht C, Fehse B, Fiedler W, Stocking C, Günther A, Mayr GW, Jücker M. (2009). Reduced proliferation of CD34(+) cells from patients with acute myeloid leukemia after gene transfer of INPP5D. Gene Ther. 16(4):570-3.

Miletic AV, Anzelon-Mills AN, Mills DM, Omori SA, Pedersen IM, Shin DM, Ravetch JV, Bolland S, Morse HC 3rd, Rickert RC. (2010). Coordinate suppression of B cell lymphoma by PTEN and SHIP phosphatases. J Exp Med. 207(11):2407-20.

Morra M, Silander O, Calpe S, Choi M, Oettgen H, Myers L, Etzioni A, Buckley R, Terhorst C. (2001). Alterations of the X-linked lymphoproliferative disease gene SH2D1A in common variable immunodeficiency syndrome. Blood. 98(5):1321-5.

Odai H, Sasaki K, Iwamatsu A, Nakamoto T, Ueno H, Yamagata T, Mitani K, Yazaki Y, Hirai H. (1997). Purification and molecular cloning of SH2- and SH3-containing inositol polyphosphate-5-phosphatase, which is involved in the signaling pathway of granulocyte-macrophage colony-stimulating factor, erythropoietin, and Bcr-Abl. Blood 89:2745-56

Pauls SD, Marshall AJ. (2017). Regulation of immune cell signaling by SHIP1: A phosphatase, scaffold protein, and potential therapeutic target. Eur J Immunol. 47(6):932-945.

Pedersen IM, Dennis Otero, Elaine Kao, Ana V Miletic, Christoffer Hother, Elisabeth Ralfkiaer, Robert C Rickert, Kirsten Gronbaek, and Michael David. (2009). Onco-miR-155 targets SHIP1 to promote TNFα-dependent growth of B cell lymphomas. EMBO Mol Med. 1(5): 288–295.

Richardson CJ, Gao Q, Mitsopoulous C, Zvelebil M, Pearl LH, Pearl FM. (2009). MoKCa database--mutations of kinases in cancer. Nucleic Acids Res. 37 (Database issue):D824-31.

Sattler M, Verma S, Byrne CH, Shrikhande G, Winkler T, Algate PA, Rohrschneider LR, Griffin JD. (1999). BCR/ABL directly inhibits expression of SHIP, an SH2-containing

polyinositol-5-phosphatase involved in the regulation of hematopoiesis. Mol Cell Biol. 19(11):7473-80.

Songyang Z, Shoelson SE, Chaudhuri M, Gish G, Pawson T, Haser WG, King F, Roberts T, Ratnofsky S, Lechleider RJ (1993). SH2 domains recognize specific phosphopeptide sequences. Cell. 72(5):767-78.

Täger M, Horn S, Latuske E, Ehm P, Schaks M, Nalaskowski M, Fehse B, Fiedler W, Stocking C, Wellbrock J, Jücker M. (2017). SHIP1, but not an AML-derived SHIP1 mutant, suppresses myeloid leukemia growth in a xenotransplantation mouse model. Gene Ther. 24(11):749-753.

Wang W, Malcolm BA. (1999). Two-stage PCR protocol allowing introduction of multiple mutations, deletions and insertions using QuikChange Site-Directed Mutagenesis. Biotechniques. 26(4):680-2.

Ware MD, Rosten P, Damen JE, Liu L, Humphries RK, Krystal G. (1996). Cloning and characterization of human SHIP, the 145-kD inositol 5-phosphatase that associates with SHC after cytokine stimulation. Blood 88:2833-40

Yang L, Luo JM, Liu XJ, Wen SP, Yang JC and Zhang JY (2009). Effects of SHIP gene mutation on cell cycle related proteins and phosphorylated Akt in K562 cells. Zhonghua Xue Ye Xue Za Zhi 30, 548-552.

Zhang SJ, Shi JY, Zhu YM, Shi ZZ, Yan-Sheng, Gu BW, Bai XT, Shen ZX, Li JY. (2006). The investigation of mutation and single nucleotide polymorphism of receptor tyrosine kinases and downstream scaffold molecules in acute myeloid leukemia. Leuk Lymphoma. 47(12):2610-6.

Figure 1: Investigation of the stability of SHIP1-F28L mutant. (A) Schematic representation of the structure of SHIP1. At the N-terminus of SHIP1 the SH2 domain (dark blue) is located. The SH2 domain contains the FLVR motif (residues 28-31; light blue). The characteristic 5-phosphatase domain of SHIP1 is centrally located (yellow). In addition, two nuclear localization signals (green), two NPXY motifs (red) and several PxxP motifs (purple) could be identified. (B) TF-1 cells were transduced with lentiviral vectors encoding SHIP1-wt, SHIP1-F28L, SHIP1-Y643H and control vector. Cells were selected after transduction with Puromycin and western blot analysis was performed (C) Three weeks after transduction, in each case RNA of transduced cells were isolated. The SHIP1 mRNA amount was determined from the respective cDNA by RT-qPCR. The determination of the relative expression of the amount of SHIP1-mRNA was carried out by normalization to the reference gene GAPDH. Specific oligonucleotides were used for transduced SHIP1 (HA-tag). In each case, mean ± standard deviation from three measurements of the respective sample is shown. (D) To investigate the recovery of SHIP1-F28L at protein level, stable SHIP1-F28L expressing TF-1 cells were treated with Src-kinase inhibitor PP2 and proteasomal inhibitor MG132. For this reason, TF-1 cells were treated for 24 h with 10 µM PP2, MG132 or DMSO. Lysates of the cells were generated by TCA precipitation. In each case 40 µg of protein lysate were separated by SDS-PAGE, proteins subsequently transferred to nitrocellulose membrane and detected with specific antibodies.

Figure 2: Investigation of the stability of SHIP1 FLVR motif mutants. To study the stability of SHIP1 mutants of the FLVR motif and putative phosphorylation sites in the immediate vicinity of the FLVR motif, H1299 cells were incubated with lentiviral particles, each vector with control vector, SHIP1-wt, SHIP1-F28L, SHIP1-F28I, SHIP1-F28V, SHIP1-F28A, SHIP1-F28Y, SHIP1-F28W and SHIP1-ΔFLVR sequence, transduced. Cells were selected after transduction with puromycin. Subsequently, protein lysates were prepared by TCA precipitation and analyzed by western blots with specific antibodies (A). (B) shows quantification of relative SHIP1 expression (B1) with corresponding quantification of relative p-AKT-S473 expression (B2) of H1299 cells. Three weeks after transduction, RNA of transduced cells was isolated. The SHIP1 mRNA amount was determined from the respective cDNA by RT-qPCR. The determination of the relative expression of the amount of SHIP1-mRNA was carried out by normalization to the reference gene GAPDH. Specific oligonucleotides were used for transduced SHIP1 (HA-tag) (C). In each case, mean ± standard deviation from three measurements of the respective sample is shown.

Figure 3: Investigation of the influence of putative phosphorylation sites in the immediate vicinity of the FLVR motif of SHIP1 on protein stability. To study the stability of SHIP1 mutants of the FLVR motif and putative phosphorylation sites in the immediate vicinity of the FLVR motif, H1299 cells were incubated with lentiviral particles, each vector with control vector, SHIP1-wt, SHIP1-K24R, SHIP1-S27A, SHIP1-S27D, SHIP1-F28L, SHIP1-L29F, SHIP1-R31Q, SHIP1-S33A, SHIP1-S33D, SHIP1-S35A, SHIP1-S35D, SHIP1-Y40A and SHIP1-Y46A sequences, transduced. Cells were selected after transduction with puromycin. Subsequently, protein lysates were prepared by TCA precipitation and analyzed by western blots with specific antibodies (A). (B) shows quantification of relative SHIP1 expression (B1) with corresponding quantification of relative p-AKT-S473 expression (B2) of H1299 cells. Three weeks after transduction, RNA of transduced cells was isolated. The SHIP1 mRNA amount was determined from the respective cDNA by RT-qPCR. The determination of the relative expression of the amount of SHIP1-mRNA was carried out by normalization to the reference gene GAPDH. Specific oligonucleotides were used for transduced SHIP1 (HA-tag) (C). In each case, mean ± standard deviation from three measurements of the respective sample is shown.

Figure 4: Analysis of the influence of SHIP1 FLVR motif mutants on growth behavior of H1299 cells. (A) To investigate the influence of SHIP1-FLVR motif mutants on growth behavior of H1299 cells, control vector, SHIP1-wt, SHIP1-F28L, SHIP1-F28W and K24R-expressing H1299 cells were seeded in triplicates at a cell density of 3×10^4 cells/well in 200 µl medium in a 96-well dish. 48 hours after seeding, addition of resazurin was used to measure the discoloration of the medium as an indicator of cell viability. (B) Using a live cell imaging analysis system, growth behavior of the cells was monitored over 24 hours. Stable SHIP1-wt, SHIP1-K24R, SHIP1-S27A, SHIP1-S27D, SHIP1-F28L, SHIP1-S33A, SHIP1-S33D, SHIP1-F28V and SHIP1-F28W expressing H1299 cells together with vector control expressing cells were each seeded in triplicates at a cell density of 3×10^4 cells/well in 100 µl medium in a 96-well dish. Statistical significance refers to control vector expressing cells (* $p \leq 0.05$; ** $p \leq 0.01$; *** $p \leq 0.001$).

Figure 5: Investigation of half-life of SHIP1-wt and SHIP1-F28L mutant in Jurkat and TF-1 cells. Half-life of SHIP1 protein was analyzed by using cycloheximide to inhibit protein synthesis. SHIP1-wt and SHIP1-F28L expressing Jurkat (A) and TF-1 (B) cells were seeded and incubated with cycloheximide or DMSO. Protein lysates were prepared as indicated at different time points. Protein lysate were separated by SDS-PAGE, proteins subsequently transferred to nitrocellulose membrane and detected with specific antibodies. The experiment was performed in triplicate. Images of representative Western blots are shown. Subsequently, expression intensity was quantified and half-life was calculated (see diagrams). Mean ± standard deviation are shown. Intensity of the Western blot bands observed at time point 0h (untreated) was set to 100%

Figure 6: Visualization of the (A) SHIP1-wt and (B) SHIP1-F28L mutant based on a SHIP1-wt NMR structure (PDB2YSX). (A) Aromatic amino acids at position 28 (F, W and Y) form hydrophobic surface contacts in particular with, W5, I83, L97 and P100. (B) The smaller-sized leucine at position 28 likely leads to a (partial) loss of these surface contacts, with significant impact on the conformation, flexibility and stability of the SH2 domain.

Figure S1: Representation of the conserved FLVR motif in SH2 domain-containing proteins. The FLVR motif (residue 28-31, according to SHIP1 sequence) or the related FLIR or YLLR motif is flanked by putative phosphorylation sites. Serine or threonine residues are often located N-terminal of the FLVR motif (residue 27). Glutamic acid / aspartic acid (residue 32) followed by a serine (residue 33) is often located C-terminal of the FLVR motif. At amino acid position 35, a serine or threonine residue is also usually found.

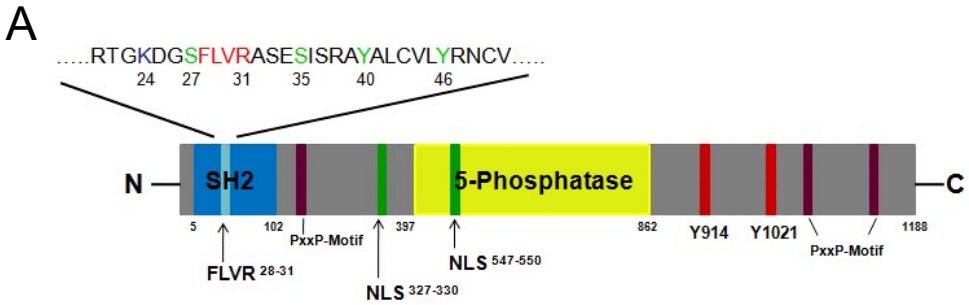
A
.....RTGKDGSFLVRASESISRAYALCVLYRNCV.....
24 27 31 35 40 46
N
SH2
5-Phosphatase
C
5
102
PxxP-Motif
397
862
Y914
Y1021
1188
PxxP-Motif
FLVR 28-31
NLS 327-330
NLS 547-550

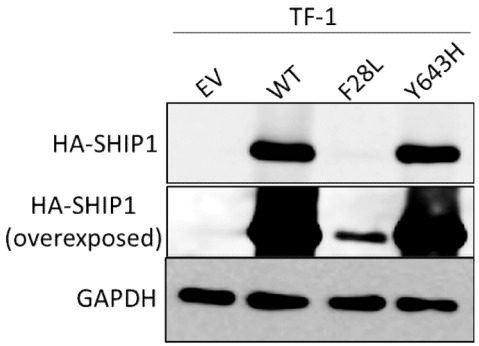
B
TF-1
EV
WT
F28L
Y643H
HA-SHIP1
HA-SHIP1
(overexposed)
GAPDH

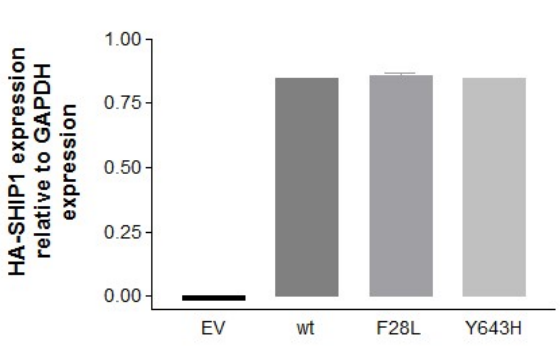
C
HA-SHIP1 expression relative to GAPDH expression
1.00
0.75
0.50
0.25
0.00
EV
wt
F28L
Y643H

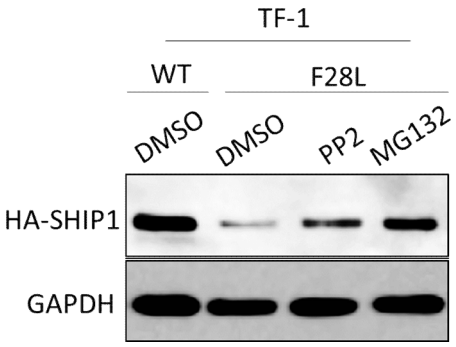
D
TF-1
WT
F28L
DMSO
DMSO
PP2
MG132
HA-SHIP1
GAPDH

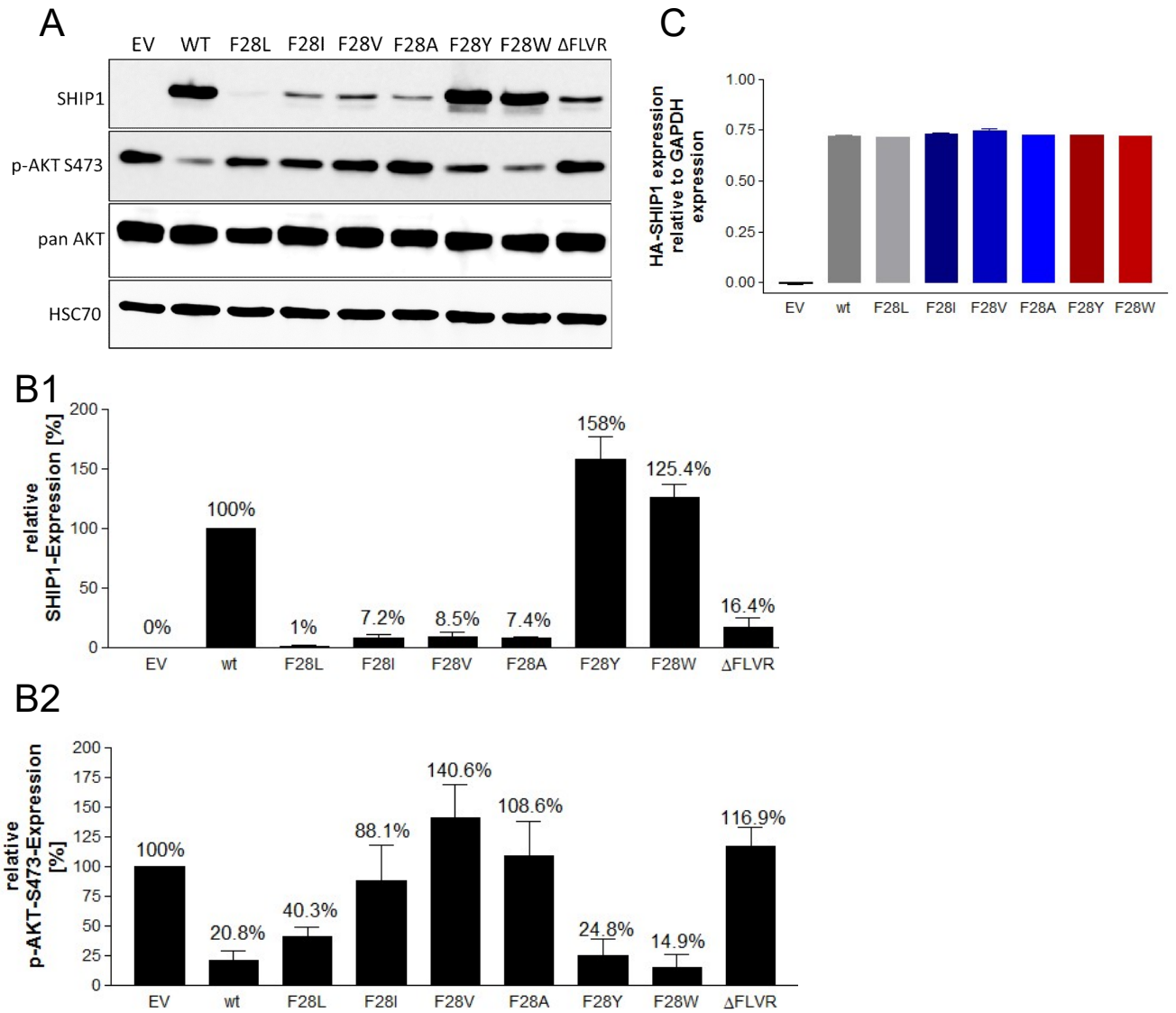
A
EV
WT
F28L
F28I
F28V
F28A
F28Y
F28W
ΔFLVR
SHIP1
p-AKT S473
pan AKT
HSC70
C
HA-SHIP1 expression relative to GAPDH expression
1.00
0.75
0.50
0.25
0.00
EV
wt
F28L
F28I
F28V
F28A
F28Y
F28W
B1
relative SHIP1-Expression [%]
200
150
100
50
0
0%
100%
1%
7.2%
8.5%
7.4%
158%
125.4%
16.4%
EV
wt
F28L
F28I
F28V
F28A
F28Y
F28W
ΔFLVR
B2
relative p-AKT-S473-Expression [%]
200
175
150
125
100
75
50
25
0
100%
20.8%
40.3%
88.1%
140.6%
108.6%
24.8%
14.9%
116.9%
EV
wt
F28L
F28I
F28V
F28A
F28Y
F28W
ΔFLVR

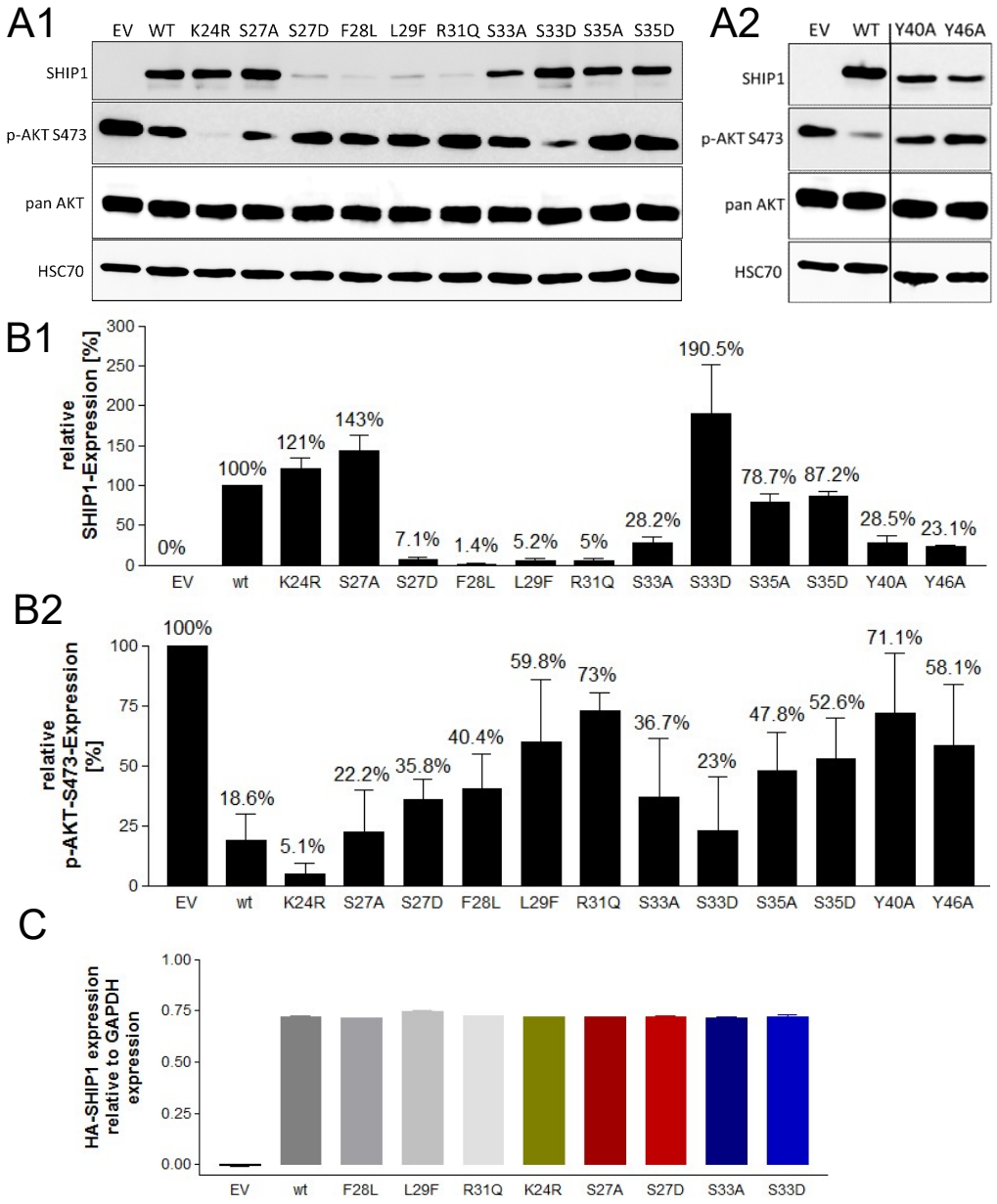
A1
EV WT K24R S27A S27D F28L L29F R31Q S33A S33D S35A S35D
SHIP1
p-AKT S473
pan AKT
HSC70
A2
EV WT Y40A Y46A
SHIP1
p-AKT S473
pan AKT
HSC70
B1
relative SHIP1-Expression [%]
0% 100% 121% 143% 7.1% 1.4% 5.2% 5% 28.2% 190.5% 78.7% 87.2% 28.5% 23.1%
EV wt K24R S27A S27D F28L L29F R31Q S33A S33D S35A S35D Y40A Y46A
B2
relative p-AKT-S473-Expression [%]
100% 18.6% 5.1% 22.2% 35.8% 40.4% 59.8% 73% 36.7% 23% 47.8% 52.6% 71.1% 58.1%
EV wt K24R S27A S27D F28L L29F R31Q S33A S33D S35A S35D Y40A Y46A
C
HA-SHIP1 expression relative to GAPDH expression
EV wt F28L L29F R31Q K24R S27A S27D S33A S33D

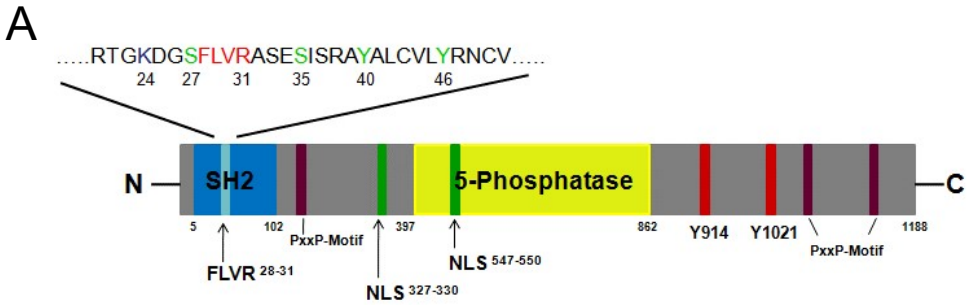
A
.....RTGKDGSFLVRASESISRAYALCVLYRNCV.....
24 27 31 35 40 46
N
SH2
5-Phosphatase
C
5
102
PxxP-Motif
397
862
Y914
Y1021
1188
PxxP-Motif
FLVR 28-31
NLS 327-330
NLS 547-550

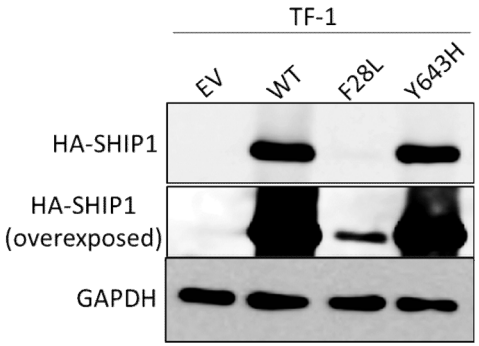
B
TF-1
EV
WT
F28L
Y643H
HA-SHIP1
HA-SHIP1
(overexposed)
GAPDH

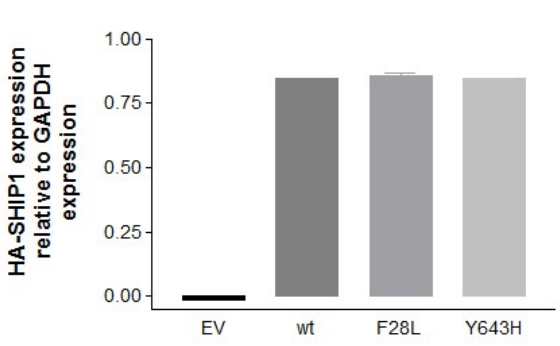
C
HA-SHIP1 expression relative to GAPDH expression
1.00
0.75
0.50
0.25
0.00
EV
wt
F28L
Y643H

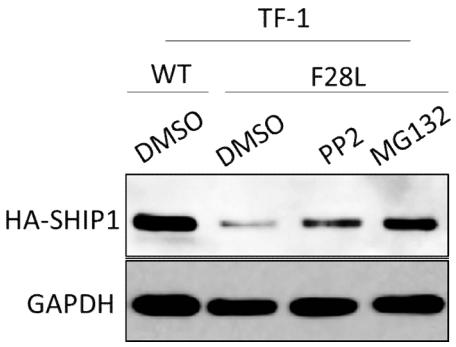
D
TF-1
WT
F28L
DMSO
DMSO
PP2
MG132
HA-SHIP1
GAPDH

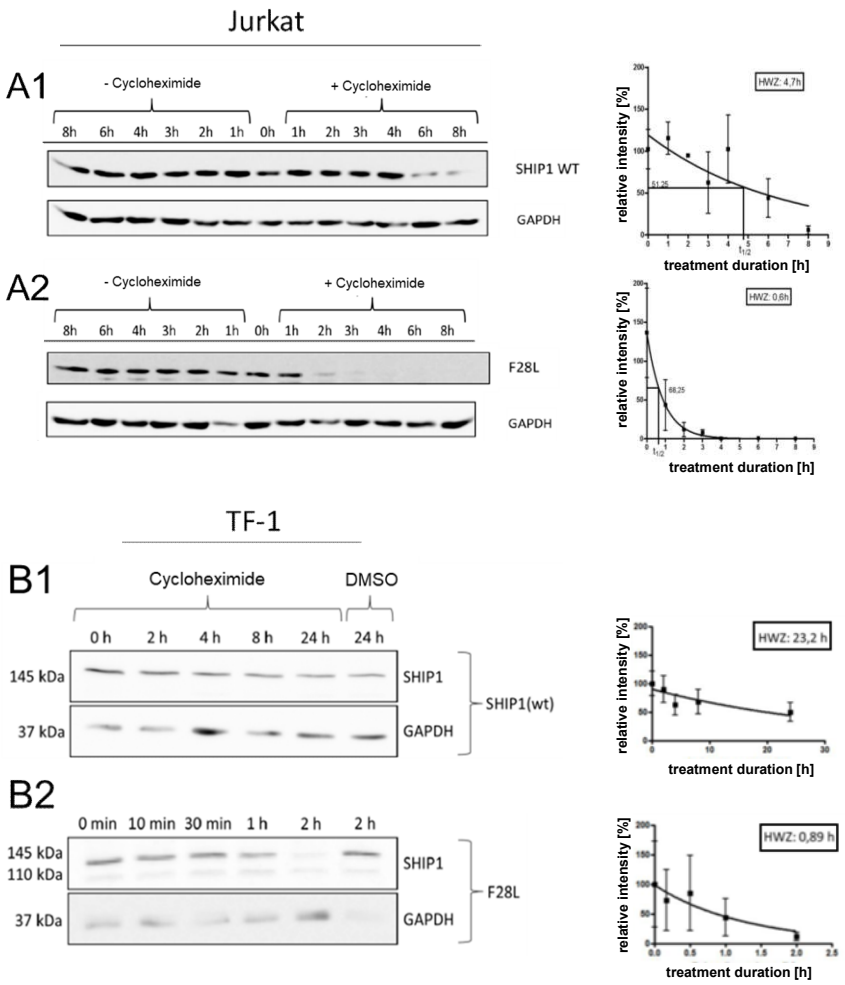
Jurkat
A1
- Cycloheximide
+ Cycloheximide
8h 6h 4h 3h 2h 1h 0h 1h 2h 3h 4h 6h 8h
SHIP1 WT
GAPDH
A2
- Cycloheximide
+ Cycloheximide
8h 6h 4h 3h 2h 1h 0h 1h 2h 3h 4h 6h 8h
F28L
GAPDH
TF-1
B1
Cycloheximide
DMSO
0 h 2 h 4 h 8 h 24 h 24 h
145 kDa
37 kDa
SHIP1
GAPDH
SHIP1(wt)
B2
0 min 10 min 30 min 1 h 2 h 2 h
145 kDa
110 kDa
37 kDa
SHIP1
GAPDH
F28L

HWZ: 4.7h
relative intensity [%]
treatment duration [h]
HWZ: 0.8h
relative intensity [%]
treatment duration [h]

HWZ: 23,2 h
relative intensity [%]
treatment duration [h]
HWZ: 0,89 h
relative intensity [%]
treatment duration [h]

A

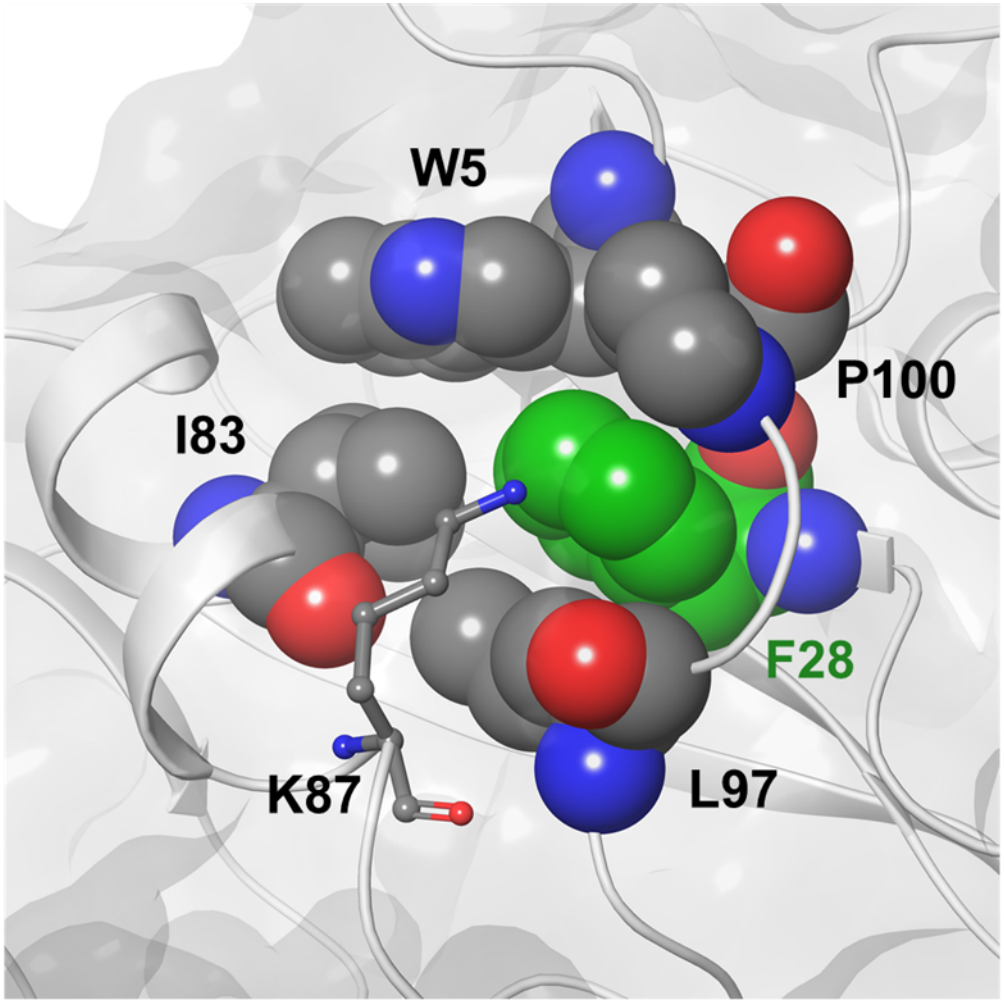

B